

# Ultimate performance of GRP-laminates under in-plane biaxial loading

G.M. Sluimer

Delft University of Technology, Department of Civil Engineering

Email: g.sluimer@ct.tudelft.nl

Widespread acceptance and utilisation of composite laminates requires confidence in their load-bearing capacity. The ability to accurately predict the stiffness and strength of laminates composed of glass-fibre reinforced polyester (GRP) is necessary for a sound design when laminates are used in structural applications.

In this paper an easily accessible computational tool has been described that is able to deal with the phenomenon of progressive failure. Because loading in structural applications is merely biaxial, we designed experiments to test the biaxial capacities of GRP-laminates. The final computational results show an excellent agreement with the biaxial test results.

*Key words:* biaxial testing, progressive failure, composite laminates, glass-fibre reinforced polyester

## 1 Introduction

One of the reasons that fibre-reinforced composite applications in building engineering are lagging behind other disciplines (like aeronautical engineering and mechanical engineering) is the lack of familiarity of many building engineers with the potential of fibre reinforced composites for structural applications.

Although present design codes often refer to the Tsai-Wu criterion, the additional advantages of anisotropy are hardly taken into account and no design tools are available to optimise the composition of multidirectional laminates. An approach where a laminate is considered failed after the first layer has failed, will not lead to the application of a sound safety-factor. This will inevitably lead to improper laminate design and uneconomical use of material.

In order to contribute to filling the above-mentioned gap, we have developed a computational tool supported by experiments that enables us to analyse the development of stresses and strains in glass-fibre reinforced polyester (GRP) laminates beyond the level of first-ply failure up to ultimate laminate failure. This approach may be referred to as progressive failure analysis.

The experiments on biaxial specimens have been simulated by the finite element method using the Ansys finite element package. An easily accessible computing method is developed in order to predict ultimate failure and at the same time giving good insight into the type of failure and the critical locations. The parameters used in the computational procedures will be adapted to a value for which a satisfactory result is achieved for different types of testing.

Since the Tsai-Wu failure criterion uses second and fourth order tensors, the linear treatment of stresses and strains in laminates using tensor-notation is summarised in chapter 2.

In chapter 3, the biaxial test set-up is described, while in chapter 4 the computational and experimental results are compared.

Finally, the design of a vertical storage vessel is worked out in chapter 5, as an example of the versatility of the proposed computational procedure.

## 2 Analysis of composite laminates

Most of the structural elements or laminates made of fibrous composites consist of several distinct layers of unidirectional laminae. Each lamina is usually made of the same constituent materials (e.g. resin and glass). However, an individual layer may differ from another layer in relative volumes of the constituent materials, type of reinforcement used, and, more particularly, orientation of fibres with respect to common reference axes. Analysis and design of any structural element will require a complete knowledge of the properties of individual layers and a lamination theory. We will use the classical lamination theory, where the constitutive behaviour of laminates is studied exclusively in the plane of the laminate. The reason for this is the fact that no delamination effects have been encountered in the experiments described in chapter 3.

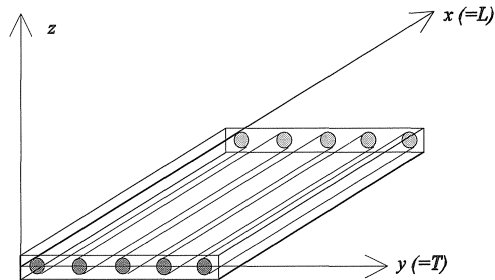


Fig. 2.1 Schematic view of uni-directional lamina and co-ordinate system.

A multidirectional laminate consists of layers with different fibre directions.

A single-layer composite represents a basic building block for laminate constructions and therefore attention is given to the properties and behaviour of unidirectional composites. A schematic view of a unidirectional lamina is depicted in Figure 2.1. The x-axis of the layer coordinate system is orientated along the fibres, while the z-axis is perpendicular to the plane of the layer. The depicted axes in the laminate plane are often referred to as L and T.

First, linear elastic behaviour is assumed, but this can easily be extended to non-linear material behaviour by substituting the appropriate relation between stresses and strains.

## 2.1 Constitutive equations of the unidirectional lamina

The constitutive equations, which describe the relationship between stresses and strains, will be set up by means of tensors, and not based on matrix calculation methods, which is common practice in the literature. The method based on tensors is straightforward and therefore easy to handle; on the other hand, special attention has to be given to the translation from tensor-elements into engineering constants.

The general linear 3-dimensional stress-strain relationship is governed by the stiffness tensor  $C_{ijkl}$  or it's inverse: the flexibility (compliance) tensor  $S_{ijkl}$ , according to Equation (2.1) and Equation (2.2).  $C_{ijkl}$  and  $S_{ijkl}$  are fourth rank tensors and  $\sigma_{ij}$  and  $\epsilon_{kl}$  are second rank ( $3 \times 3$ ) tensors. The indices refer to the co-ordinate axes ( $1 = x$ ) etc. and adopt values  $i, j, k, l = 1...3$ .

$$\sigma_{ij} = C_{ijkl} \cdot \epsilon_{kl} \quad (2.1)$$

$$\epsilon_{ij} = S_{ijkl} \cdot \sigma_{kl} \quad (2.2)$$

In both equations, the Einstein-convention is valid, thus summation over the repeated indices has to be performed. Choosing the co-ordinate system parallel to the material symmetry axes, the material tensors can be simplified, because then there is no relation between normal stresses and shear strains or between normal strains and shear stresses (special orthotropy).

For the orthotropic unidirectional layer, the fully worked-out equations, related to the principal material axes of the unidirectional layer, are expanded in Equation (2.3).

In order to define the coefficients of the stiffness tensor and the compliance tensor in terms of the engineering elastic constants  $E$ ,  $\nu$  and  $G$ , a conversion to engineering notation has to be made.

The conventions that have to be used are listed in Table 2.1.

$$\begin{pmatrix} \epsilon_{11} \\ \epsilon_{22} \\ \epsilon_{33} \\ \epsilon_{23} \\ \epsilon_{32} \\ \epsilon_{13} \\ \epsilon_{31} \\ \epsilon_{12} \\ \epsilon_{21} \end{pmatrix} = \begin{bmatrix} s_{1111} & s_{1122} & s_{1133} & 0 & 0 & 0 & 0 & 0 & 0 \\ s_{2211} & s_{2222} & s_{2233} & 0 & 0 & 0 & 0 & 0 & 0 \\ s_{3311} & s_{3322} & s_{3333} & 0 & 0 & 0 & 0 & 0 & 0 \\ 0 & 0 & 0 & s_{2323} & s_{2332} & 0 & 0 & 0 & 0 \\ 0 & 0 & 0 & s_{3223} & s_{3232} & 0 & 0 & 0 & 0 \\ 0 & 0 & 0 & 0 & 0 & s_{1313} & s_{1331} & 0 & 0 \\ 0 & 0 & 0 & 0 & 0 & s_{3113} & s_{3131} & 0 & 0 \\ 0 & 0 & 0 & 0 & 0 & 0 & 0 & s_{1212} & s_{1221} \\ 0 & 0 & 0 & 0 & 0 & 0 & 0 & s_{2112} & s_{2121} \end{bmatrix} \cdot \begin{pmatrix} \sigma_{11} \\ \sigma_{22} \\ \sigma_{33} \\ \sigma_{23} \\ \sigma_{32} \\ \sigma_{13} \\ \sigma_{31} \\ \sigma_{12} \\ \sigma_{21} \end{pmatrix} \quad (2.3)$$

Table 2.1 Tensor versus contracted and engineering notation for stresses and strains.

Stresses			Strains		
Tensor notation	Contracted notation	Engineering notation	Tensor notation	Contracted notation	Engineering notation
$\sigma_{11}$	$\sigma_1$	$\sigma_1$	$\epsilon_{11}$	$\epsilon_1$	$\epsilon_1$
$\sigma_{22}$	$\sigma_2$	$\sigma_2$	$\epsilon_{22}$	$\epsilon_2$	$\epsilon_2$
$\sigma_{33}$	$\sigma_3$	$\sigma_3$	$\epsilon_{33}$	$\epsilon_3$	$\epsilon_3$
$\sigma_{23} = \sigma_{32}$	$\sigma_4$	$\tau_{23} = \tau_{32}$	$\epsilon_{23} = \epsilon_{32}$	$\frac{1}{2} \epsilon_4$	$\frac{1}{2} \gamma_{23}$
$\sigma_{13} = \sigma_{31}$	$\sigma_5$	$\tau_{13} = \tau_{31}$	$\epsilon_{13} = \epsilon_{31}$	$\frac{1}{2} \epsilon_5$	$\frac{1}{2} \gamma_{13}$
$\sigma_{12} = \sigma_{21}$	$\sigma_6$	$\tau_{12} = \tau_{21}$	$\epsilon_{12} = \epsilon_{21}$	$\frac{1}{2} \epsilon_6$	$\frac{1}{2} \gamma_{12}$

Using the contracted notation, Equation (2.2) can be rewritten as:

$$\epsilon_i = S_{ij} \cdot \sigma_j \quad (2.4)$$

The elements of the flexibility tensor  $S_{ijkl}$  can be expressed in the engineering constants. Special attention has to be given to the expression of the shear coefficients, illustrated by Equation (2.5) to Equation (2.7).

$$\epsilon_{12} = s_{1212} \cdot \sigma_{12} + s_{1221} \cdot \sigma_{21} \quad (2.5)$$

$$\epsilon_{21} = s_{2112} \cdot \sigma_{12} + s_{2121} \cdot \sigma_{21} \quad (2.6)$$

It follows from  $\epsilon_{12} = \epsilon_{21}$  (by definition) that and  $s_{1212} = s_{2112}$  and  $s_{1221} = s_{2121}$ .

Because of Maxwell symmetry:  $s_{1221} = s_{2112}$ , so  $s_{1212} = s_{1221} = s_{2112} = s_{2121}$ . So, Equation (2.5) and Equation (2.6) can be converted to engineering notation as follows:

$$\gamma_{12} = \epsilon_{12} + \epsilon_{21} = 4s_{1212} \tau_{12} \quad (2.7)$$

from which it can be seen that the engineering shear modulus  $G_{12} = \frac{1}{4s_{1212}}$ , and that  $G_{12} = G_{21}$ , etc.

The full compliance tensor in material symmetry directions expressed in the engineering constants can be written according to Equation 2.8.

$$S_{ijkl} = \begin{bmatrix} \frac{1}{E_1} & -\frac{\nu_{21}}{E_2} & -\frac{\nu_{31}}{E_3} & 0 & 0 & 0 & 0 & 0 & 0 \\ -\frac{\nu_{12}}{E_1} & \frac{1}{E_2} & -\frac{\nu_{32}}{E_3} & 0 & 0 & 0 & 0 & 0 & 0 \\ -\frac{\nu_{13}}{E_3} & -\frac{\nu_{23}}{E_2} & \frac{1}{E_3} & 0 & 0 & 0 & 0 & 0 & 0 \\ 0 & 0 & 0 & \frac{1}{4G_{23}} & \frac{1}{4G_{23}} & 0 & 0 & 0 & 0 \\ 0 & 0 & 0 & \frac{1}{4G_{23}} & \frac{1}{4G_{23}} & 0 & 0 & 0 & 0 \\ 0 & 0 & 0 & 0 & 0 & \frac{1}{4G_{13}} & \frac{1}{4G_{13}} & 0 & 0 \\ 0 & 0 & 0 & 0 & 0 & \frac{1}{4G_{13}} & \frac{1}{4G_{13}} & 0 & 0 \\ 0 & 0 & 0 & 0 & 0 & 0 & 0 & \frac{1}{4G_{12}} & \frac{1}{4G_{12}} \\ 0 & 0 & 0 & 0 & 0 & 0 & 0 & \frac{1}{4G_{12}} & \frac{1}{4G_{12}} \end{bmatrix} \quad (2.8)$$

It can be derived from symmetry that  $S_{ijkl} = S_{klij}$ . This relation can be used for instance to express the minor Poisson's ratios into the major Poisson's ratios, for instance:

$$\nu_{12} = \frac{E_1}{E_2} \nu_{21}.$$

Application of the full tensor notation, with coefficients using four indices in the case of a fourth order tensor, is necessary in order to transform stresses and strains in terms of a rotated co-ordinate system, see Equation (2.10).

The stiffness tensor of the unidirectional lamina is the inverse of the flexibility tensor.

The stiffness tensor of a multi-directional laminate will be determined by addition of the stiffness components of the composing layers. The procedure that has to be followed will be explained in general in the next section.

The corresponding treatment for the stiffness tensor  $C_{ijkl}$  is very similar.

## 2.2 Analysis of multi-directional laminates

Structural composites usually consist of several anisotropic plies bonded together at different orientations, because a unidirectional laminate is not very effective due to the low strength and stiffness perpendicular to the fibre direction.

The stiffness tensor  $C$  of a multi-directional laminate can be found by adding (proportional with thickness) the stiffness tensors of the composing layers; the stiffness tensor for each layer must therefore be transformed to the same co-ordinate axis. Because the compliance tensor in the fibre direction is related to the engineering constants according to Equation (2.8), these tensors have to be transformed to the same direction, and subsequently be inverted to the stiffness tensor for that particular direction.

Finally, considering the individual thickness of the composing layers, the stiffness tensors of the individual layers can be added, resulting in the stiffness tensor of the multi-directional laminate:

$$C_{lam}^x = \sum_{i=1}^n \frac{C_i^x \cdot t_i}{t_{lam}} \quad (2.9)$$

The procedure described above is based on the condition that the strain conditions are the same for each individual layer.

The compliance tensor  $S_{ijkl}$  of the laminate can be derived by inverting the stiffness tensor  $C_{ijkl}$ .

With the compliance tensor in fibre direction as a starting-point, the coefficients of the compliance tensor in an arbitrary direction can be determined following the general rotation equation for fourth order tensors:

$$\bar{s}_{ijkl} = a_{im}a_{jn}a_{ko}a_{lp} \cdot s_{mnop} \quad (2.10)$$

where  $a_{im}$  etc. are the cosine of the angle between the  $i$ -axis after rotation, and the  $m$ -axis before rotation. To evaluate the tensor-equation, the 'Einstein'-convention, meaning summation over the repeated indices has to be used again.

In the particular case of a plane stress situation, the stress-strain relationship for the engineering constants can be expressed in a  $3 \times 3$  matrix according to Equation (2.11) in any arbitrary direction. At the same time, we switch to contracted indices of the coefficients of the flexibility matrix and of the extensional stress and strain components.

$$\begin{Bmatrix} \bar{\epsilon}_1 \\ \bar{\epsilon}_2 \\ \bar{\gamma}_{12} \end{Bmatrix} = \begin{bmatrix} \bar{s}_{11} & \bar{s}_{12} & \bar{s}_{16} \\ \bar{s}_{21} & \bar{s}_{22} & \bar{s}_{26} \\ \bar{s}_{61} & \bar{s}_{62} & \bar{s}_{66} \end{bmatrix} \cdot \begin{Bmatrix} \bar{\sigma}_1 \\ \bar{\sigma}_2 \\ \bar{\tau}_{12} \end{Bmatrix} \quad (2.11)$$

For each individual layer of a multidirectional laminate, the compliance tensor will be determined in a particular direction by using the rotation angle of that layer. The coefficients of the compliance tensor are thereby expressed along the axes of material symmetry.

By way of example we will work out this procedure for a balanced cross-ply laminate (symmetric lay-up and equal thickness in both fibre directions) loaded in the  $45^\circ$ -direction as shown in Figure 2.2.

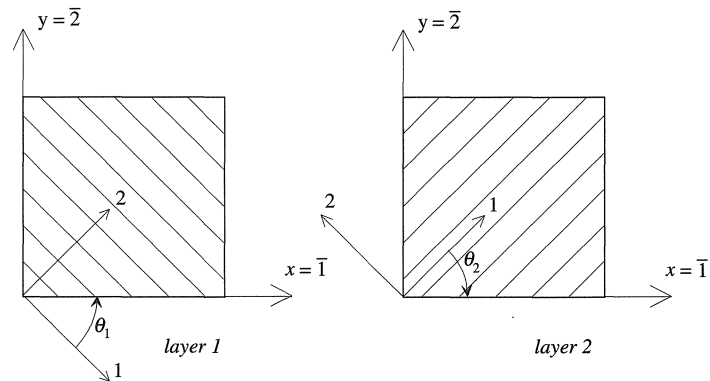


Fig. 2.2. Unidirectional laminae.

This will result in a relationship between the shear modulus of the individual layer  $G_{LT}$  and the modulus of elasticity ( $E_x$ ) and the Poisson's ratio of the cross-ply laminate in the  $45^\circ$  direction ( $\nu_{xy}$ ). In terms of the rotation angle  $\theta$ ,  $\bar{s}_{11}$  and  $\bar{s}_{21}$  can be expressed as follows, using Equation (2.10):

$$\bar{s}_{11} = s_{11}\cos^4\theta + s_{22}\sin^4\theta + (2s_{12} + s_{66})\cos^2\theta\sin^2\theta \quad (2.12)$$

$$\bar{s}_{12} = (s_{11} + s_{22} - s_{66})\cos^2\theta\sin^2\theta + s_{12}(\cos^4\theta + \sin^4\theta) \quad (2.13)$$

Clearly, the expressions for  $\bar{s}_{11}$  and  $\bar{s}_{12}$  yield the same result for  $\theta_1 = +45^\circ$  and  $\theta_2 = -45^\circ$ . It follows from Equation (2.12) and Equation (2.13) that in the directions rotated over  $45^\circ$  (coinciding with the  $xy$ -system) for both layers:

$$\bar{s}_{11} = \frac{1}{4}(s_{11} + s_{22}) + \frac{1}{2}s_{21} + \frac{1}{4}s_{66} \quad (2.14)$$

$$\bar{s}_{21} = \frac{1}{4}(s_{11} + s_{22}) + \frac{1}{2}s_{21} - \frac{1}{4}s_{66} \quad (2.15)$$

Subtraction of the two equations above results in:

$$\bar{s}_{11} - \bar{s}_{21} = \frac{1}{2}s_{66} \quad (2.16)$$

This can be rewritten in engineering constants:

$$G_{LT} = \frac{E_x}{2(1 + \nu_{xy})} \quad (2.17)$$

So, for symmetric ( $+45^\circ$ ,  $-45^\circ$ ) laminates, Equation (2.17) can be used to determine the shear modulus, if  $E_x$  and  $\nu_{xy}$  are known.

The laminate strains  $\{\varepsilon\}$  at any distance from the middle surface are given by:

$$\{\varepsilon\} = \{\varepsilon^0\} + z\{\kappa\} \quad (2.18)$$

where  $\{\varepsilon^0\}$  represents the midplane (membrane) strain and  $\kappa_x$ ,  $\kappa_y$  and  $\kappa_{xy}$  are the components of curvature.

For laminates with a non-symmetric stacking order, the forces and moments on a unit square out of the flat shell can be defined as:

$$\begin{Bmatrix} N \\ M \end{Bmatrix} = \begin{bmatrix} A & B \\ B & D \end{bmatrix} \begin{Bmatrix} \varepsilon^0 \\ \kappa \end{Bmatrix} \quad (2.19)$$

where:

$$(A_{ij}; B_{ij}; D_{ij}) = \int_{-h/2}^{h/2} \bar{c}_{ij}^k(1, z, z^2) dz \quad (2.20)$$

are the extensional, coupling and bending laminate stiffness-tensors.  $N$  and  $M$  are the resultant force and moment vectors acting per unit of length of the laminate, i.e.,

$$(N_x, N_y, N_{xy}; M_x, M_y, M_{xy}) = \int_{-h/2}^{h/2} (\sigma_x^k, \sigma_y^k, \sigma_{xy}^k; z \sigma_x^k, z \sigma_y^k, z \sigma_{xy}^k) dz \quad (2.21)$$

It is worthwhile to note that, analytically, the composing layers of a laminate are assumed homogeneous.

### 2.3 Failure mechanics of an orthotropic layer

#### 2.3.1 Tsai-Wu failure criterion

To predict failure in an orthotropic layer, use can be made of a number of failure criteria.

We will use the Tsai-Wu failure criterion to predict not only first-ply failure, but ply failure in each stage of damage. After initiation of failure, the deformation properties will be changed but the material will still be capable to carry a considerable load.

A very general failure criterion can be postulated by a power-function of the cubic, quadratic and linear scalar products:

$$[F_{ijk} \sigma_i \sigma_j \sigma_k]^\alpha + [F_{ij} \sigma_i \sigma_j]^\beta + [F_i \sigma_i]^\gamma = 1 \quad (2.22)$$

where  $\sigma_i (i, j, k = 1 \dots 6)$  is a general 3-dimensional state of stress and  $F_{ijk}$ ,  $F_{ij}$  and  $F_i$  are tensors using the contracted notation (see Table 2.1). The orientation of the co-ordinate axes may be chosen arbitrary.

The Tsai-Wu failure criterion is a simplified case of the general criterion, where the cubic term has vanished and the exponents for the quadratic and linear terms are set to unity, resulting in:

$$F_{ij} \cdot \sigma_i \cdot \sigma_j + F_i \cdot \sigma_i = 1 \quad (i, j = 1 \dots 6) \quad (2.23)$$

The strength of an orthotropic or transversely isotropic ply under plane stress relative to the symmetry-axes 1-2 should be unaffected by the direction or sign of the shear stress component. Thus, all terms in Equation (2.23) containing first-degree shear stress must be deleted from the equation. From this symmetry-consideration it follows that the strength parameters  $F_{16}$ ,  $F_{26}$  and  $F_6$  equal zero.

The general criterion can now be expanded to:

$$F_{11} \cdot \sigma_1^2 + 2F_{12} \cdot \sigma_1 \cdot \sigma_2 + F_{22} \cdot \sigma_2^2 + F_{66} \cdot \sigma_6^2 + F_1 \cdot \sigma_1 + F_2 \cdot \sigma_2 = 1 \quad (2.24)$$

where  $(\sigma_1, \sigma_2, \sigma_6)$  is a limit stress situation related to the symmetry directions.

$F_i$  and  $F_{ij}$  can be expressed in the unidirectional critical stresses which can be derived from uniaxial experiments:

$$F_{11} = \frac{1}{X_t X_c}, F_{22} = \frac{1}{Y_t Y_c}, F_{66} = \frac{1}{S^2}$$

$$F_1 = \frac{1}{X_t} + \frac{1}{X_c}, F_2 = \frac{1}{Y_t} + \frac{1}{Y_c},$$

where  $X_t$  and  $X_c$  represent the tensile and compressive strength in the 1-direction,  $Y_t$  and  $Y_c$  the tensile and compressive strength in the 2-direction, respectively, and  $S$  represents the shear strength.

The coefficient  $F_{12}$  of the second term in Equation (2.24), interpreting the interaction of the extensional stresses, can be written as  $F_{12} = F_{12}^* \sqrt{F_{11} F_{22}}$ , with  $F_{12}^*$  dimensionless.

The stress envelopes represented by Equation (2.24) will be closed, if the following condition for  $F_{12}^*$  is satisfied:  $-1 \leq F_{12}^* \leq 1$ .

It is worthwhile to note that the expressions  $F_i$  and  $F_{ij}$  are related to the orthogonal material directions. To determine the values for  $F_i$  and  $F_{ij}$  in other directions, the tensors have to be transformed to those directions.

By way of example, the permissible load space typical for unidirectional laminates is depicted in Figure 2.3 for fibre directions  $\theta_1 = 0^\circ$  and  $\theta_2 = 15^\circ$ .

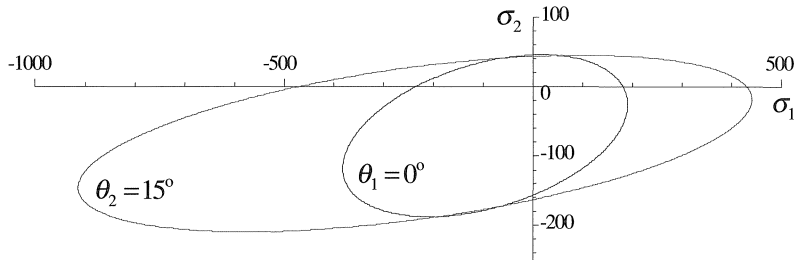


Fig. 2.3 Tsai-Wu failure curves for a unidirectional composite with fibre direction  $\theta_1 = 0^\circ$  or  $\theta_2 = 15^\circ$ . (stresses in MPa).

### 2.3.2 Puck's criterion

Failure in composite laminates is complicated because fibres and matrix has its own failure behaviour and characteristics. Puck's criterion comprises failure phenomena in both constituents. Considering physical failure phenomena occurring in unidirectional fibre reinforced materials, there are two different types of failure, namely:

- Fibre failure in tension and in compression (micro-buckling) respectively
- Matrix failure and matrix-fibre bond failure, for which the Von Mises criterion can be applied

For a unidirectional laminate with fibres in the x-direction under general loading  $(\sigma_x, \sigma_y, \tau_{xy})$ , the stresses in the matrix material are:

$$(\sigma_x)_m = \varepsilon_m \cdot E_m \approx \sigma_x \frac{E_m}{E_f \nu_f} \quad (2.25)$$

$$(\sigma_y)_m \approx \sigma_y \quad (2.26)$$

$$(\tau_{xy})_m \approx \tau_{xy} \quad (2.27)$$

Substituting these values in the Von Mises criterion yields:

$$\left( \frac{\sigma_x}{\sigma_{yu} \nu_f E_f / E_m} \right)^2 + \left( \frac{\sigma_y}{\sigma_{yu}} \right)^2 + \left( \frac{\tau_{xy}}{\tau_{xyu}} \right)^2 - \frac{\sigma_x \sigma_y}{\sigma_{yu}^2 \nu_f E_f / E_m} \leq 1 \quad (2.28)$$

Because  $E_f/E_m \gg 1$ , the first and the last term can be neglected, and we obtain Puck's criterion for fibre failure and matrix failure respectively:

$$\frac{\sigma_x}{\sigma_{xu}} \leq 1 \quad (2.28a)$$

$$\left( \frac{\sigma_x}{\sigma_{yu}} \right)^2 + \left( \frac{\tau_{xy}}{\tau_{xyu}} \right)^2 \leq 1 \quad (2.28b)$$

We will apply a modified Puck's criterion as a selective tool to determine analytically the type of failure in a ply of a multidirectional laminate.

#### 2.4 Progressive damage model

The mechanisms for damage progression and accumulation in laminated composites containing stress concentrations are extremely complicated. They are a combination of matrix cracking, fibre/matrix splitting, fibre breakage and delamination, etc. It is also critical in the design of a composite to be able to select criteria that can appropriately handle damage phenomena and to predict residual strengths of the laminates after they have been preloaded beyond the initial failure level.

Our approach is to use the Tsai-Wu criterion to find the critical stress combination in a multi-layer laminate. This failure criterion will be applied to the actual material constitution, taking into account the degraded material properties like stiffness and strength.

The computed stresses are used to determine the mode of failure.

The stress level relative to the ultimate stress in the fibre direction and perpendicular to the fibres, defined through  $\Pi_1$  and  $\Pi_2$  in Equation (2.29) and Equation (2.30), has to be compared. (Notice the differences for tensile and compressive stresses)

To determine the type of failure,

$$\Pi_1 = \frac{\sigma_1}{X_t} \quad (\sigma_1 \geq 0); \quad \Pi_1 = \frac{\sigma_1}{X_c} \quad (\sigma_1 < 0) \quad (2.29)$$

$$\Pi_2 = \sqrt{\left(\frac{\sigma_2}{Y_t}\right)^2 + \left(\frac{\sigma_6}{S}\right)^2} \quad (\sigma_2 \geq 0); \quad \Pi_2 = \sqrt{\left(\frac{\sigma_2}{Y_c}\right)^2 + \left(\frac{\sigma_6}{S}\right)^2} \quad (\sigma_2 < 0) \quad (2.30)$$

The selective criterion that we will use resembles Puck's criterion, except that only one particular type of failure can occur simultaneously at a specific load level. For this purpose, we use the multiplying factor  $\beta$  as a selective parameter. If  $\Pi_1 > \beta \cdot \Pi_2$  we will assume fibre failure occurs. In the opposite case ( $\Pi_1 \leq \beta \cdot \Pi_2$ ), we will assume matrix failure occurs.

A proper value for parameter  $\beta$  will be determined in accordance with the experimental results.

The procedure to analyse progressive failure consists of a number of sub-procedures that has to be followed:

- i. Generation of a finite element model
- ii. First solving step and determination of first-ply failure
- iii. Modification of elements and repeated solving steps
- iv. Output of results

The first important step is the generation of the finite element model in Ansys 5.3, the choice of type of element (shell91), the element key options (element geometry, number of layers, output options, etc.) and the definition of material properties.

Most important for the proposed procedure of analysing progressive failure are the degraded properties of the applied materials in different stages of damage. Because we will apply classical lamination theory, we can restrict the material properties to the in-plane stiffness, Poisson's ratios and strengths for the following material types:

Material-1 is undamaged material.

Material-2 is damaged by matrix failure along the direction of the fibres. The properties in the fibre direction are not changed compared with material-1, and perpendicular to the fibres we will reduce stiffness to zero.

Material-3 is defined as completely failed: the stiffness equals zero and the strength values are set values that are one order of magnitude greater. This means that when applying the Tsai-Wu failure criterion to the failed layer, failure will not be found again for the same layer.

First, a unit load is applied to the finite element model. After the problem has been solved, the inverse safety factor  $\xi_3 = 1/Sf$  is determined for each element, according to the Tsai-Wu failure criterion. The inverse of the determined maximum for  $\xi_3$  equals the minimum safety factor of the laminate. The unit load multiplied with this value for the safety factor, is the load that has to be applied to the structure in order to find a critical value for the Tsai-Wu criterion. Therefore, at this level of loading first-ply failure will computationally occur.

A reiterative procedure will be followed to accomplish a gradually degrading of the model until ultimate failure will have been reached.

The stresses in the integration points of the critical element layer are used as input for the Tsai-Wu criterion. The stresses in the normative integration point are used as input for the modification procedure.

Dependent on the actual material number of the critical layer and the result of the comparative criterion based on Equation (2.29) and Equation (2.30), the material will be modified.

The adjusted finite element model will be solved first in order to determine the external loading that has to be applied to reach the next occurrence of a critical layer. At the same time, the condition of external loading equal to or greater than external loading in the previous solving step must be fulfilled.

Solving the model with this external loading followed by material modification concludes the iterative solving procedure.

### 3 Biaxial test set-up

Because of the experimental potential of the laboratory, we have chosen a test set-up based on the flat plate method, where loading can be applied in two mutually perpendicular directions.

A variety of biaxial states of stress (in the tension-tension stress space) can be achieved by rotating the principal material axes with respect to the loading directions.

The flat plate specimen is often a square plate, subjected to tension-tension loading on its sides introduced via fibreglass tabs.

Testing a specimen based on a square plate turned out to be unsuccessful. Premature failure of the tabs occurred in the transition region of loading and in the corners of the specimen.

To avoid these problems, the specimen geometry has been changed to the geometry depicted in Figure 3.1.

Outside the inner circular area (with a 100 mm diameter), extra laminate thickness was applied, enabling the introduction of heavy loads via the pinholes.

Preliminary experiments on a specimen provided with a stress coating at the inner circular part of the specimen (shaded area in Figure 3.1), showed that a homogeneous stress field had been established in the main part of that area.

Despite this specimen configuration, failure was still initiated at the outside corners. Applying edge reinforcements, such as attached aluminium plates, could not solve this problem.

The solution was to apply a small hole in the centre of the specimen. The radius of the hole was chosen small enough so as not to disturb too much the stress-homogeneity of the centre area.

Moreover, we achieved with the small radius that the stresses along the edge of the hole are of a higher level than at the outside edges of the corner regions.

A specific advantage of testing notched biaxial specimen is that a particular laminate lay-up under investigation is loaded with a great variety of states of stress.

The most critical combination of the state of stress and the orientation of the laminate with respect to the edge of the hole will result in initiation of failure.

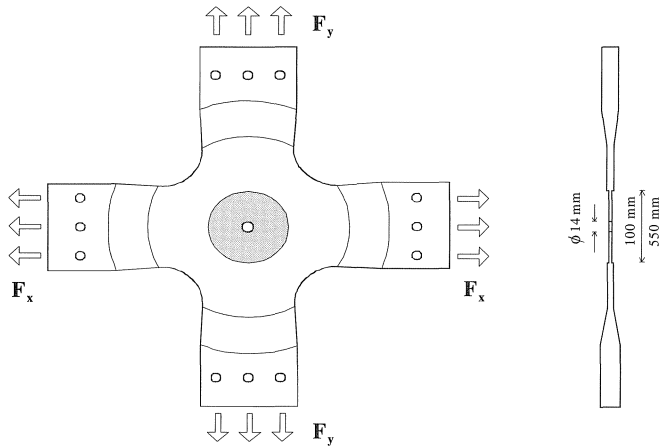


Fig. 3.1 Biaxial loaded specimen.

Order of magnitude of ultimate  $F_x$  is approximately 50 kN.

The test set-up consists of two perpendicular intersecting loading-frames. One of the frames is suspended from a four-meter high portal, allowing horizontal displacements. These horizontal displacements will cause reaction forces at the clamped specimen due to gravity. However, because of the height of the suspension portal and the limited displacement, the reaction forces are negligible.

In each frame, a hydraulic closed loop system has been installed, consisting of a hydraulic jack and a load cell. Both systems are controlled with one function generator allowing for a constant loading ratio. The signal of the load cells is generated by built-in strain gauges. These strain gauge readings are subsequently used for recording the exact loads applied to the specimen and as feedback signals for controlling the pressures by means of the servo-hydraulic system used.

In order to avoid out-of-plane bending of the specimen during loading, the laminate should be symmetric with respect to the stacking sequence. To avoid in-plane rotation, the direction of loading was restricted to the symmetry directions of the laminate.

The biaxial tests have been performed in a load-controlled manner, while the ratio of forces in both the x- and y-direction was kept constant.

Strain values were monitored by means of strain gauges in symmetry directions, applied as close as possible to the edge of the hole. The local material stresses can be derived from the appropriate material stiffness, determined by uniaxial tests.

Because of good agreement between the measured strains and average computational results over the length of the strain gauges, the use of strain gauges was abandoned later.

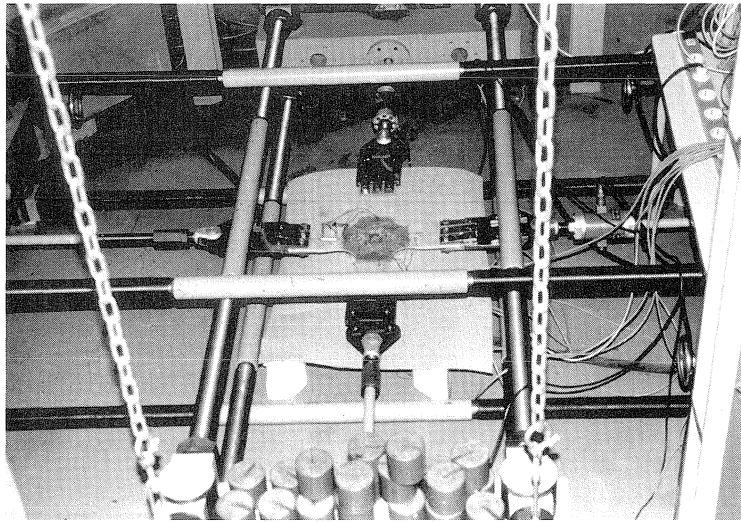


Fig. 3.2 Biaxial loading frames.

The main part of the experimental research is the biaxial loading of specimens with a variety of laminate lay-ups: type A, B, C, D, E and F (see Table 3.1).

All these laminates are composed of eight layers, consisting of unidirectionally reinforced glass-fibre polyester.

Table 3.1 Survey of laminate types.

Type	laminate lay-up	
A	$(+45^\circ, 0^\circ, -45^\circ, 0^\circ)_s$	(s = symmetrical)
B	$(+45^\circ, -45^\circ, 0^\circ, 0^\circ)_s$	(Type A and type B are identical except for the stacking sequence)
C	$(+45^\circ, -45^\circ, +45^\circ, -45^\circ)_s$	
D	$(0^\circ, 0^\circ, 0^\circ, 0^\circ)_s$	
E	$(90^\circ, 90^\circ, 90^\circ, 90^\circ)_s$	
F	$(0^\circ, 90^\circ, 0^\circ, 90^\circ)_s$	

The biaxial test results are summarised in Table 3.2 for laminate type A; individual test results are grouped together in the order of a decreasing  $F_y/F_x$ -ratio.

The values of the forces  $F_x$  and  $F_y$  listed are the values registered at ultimate failure. Parameter  $\alpha$  ( $0 < \alpha < 1$ ) equals the  $F_y/F_x$ -ratio. So,  $\alpha$  measures the extent of the bi-axiality of the loading.

Table 3.2 Biaxial test results and group averages for type A laminate.

Group	$\alpha$	Average $F_x$ [kN]	Average $F_y$ [kN]
A1	0.976	25.420	24.810
A2	0.492	45.030	22.175
A3	0.453	47.260	21.410
A4	0.410	53.080	21.770
A5	0.374	51.200	19.170
A6	0.334	49.923	16.705
A7	0.254	52.000	13.210
A8	0.103	43.560	4.477
A9	0.078	40.750	3.175
A10	0.055	42.620	2.330

## 4 Computational versus experimental results

The final goal of our approach is to be able to reliably predict the behaviour of multi-layer composites under various loading conditions. To that end, we have developed a computational tool, enabling the establishment of a sound and optimal design for composite laminates. The central issue of the computational tool is the monitoring of successive failure of separate layers according to the Tsai-Wu criterion.

The proposed procedure has been simulated with the Ansys finite element package. The computational method as developed, implicitly needs a number of parameters that have to be set to proper values in order to follow the results of the biaxial experiments as closely as possible.

The dimensioning of the biaxial specimen was realised in such a way that ultimate failure initiated at the inside hole of the central circular area of the specimen. Within a test series with the same type of laminate and loading ratio in the x- and y-direction, little scatter was found in the ultimate loading data where final rupture was reached. So the conclusion is justified that the test set-up, as well as the specimen configuration, are representative.

Moreover, we observed no delamination phenomena along the edge of the inside hole despite the fact that failure initiated at this location.

From these facts, it may be concluded that there is a minimal effect of normal out-of-plane stresses at the edge of the hole. Therefore, we think the application of classical lamination theory is justified for our specimen dimensions, choice of material and test set-up.

The main objective is to find out, whether the described computational method is capable of simulating the mechanical behaviour of multi-layer composites in laboratory testing and of finding the most appropriate parameters.

In order to achieve this goal, the proposed computational procedure will be performed for a number of laminate types and different loading ratios in the two loading directions, coinciding with the variations applied during biaxial testing.

The results will be used as a reference for the input parameters involved in the prediction of different stages of damage, such as first-ply failure, first-fibre failure and ultimate laminate failure. The analyses are performed on a precise model of the biaxial specimen. The mesh refinement that we used is high enough to get reliable results within an acceptable computation time.

The main parameters involved in the computational analyses can be divided into model parameters, analysis parameters and material parameters:

1. Model parameters:
  - refinement of the finite element mesh, parameter  $mf$
  - element type, *shell91*
2. Elastic material properties of undamaged and damaged material:
  - material type number 1 is undamaged
  - material type number 2 failed by matrix cracking
  - material type number 3 failed by fibre breakage
3. Failure criterion parameters:
  - material strength properties ( $X_v$ ,  $Y_v$ ,  $S_v$  etc.)
  - further coefficients  $F_i$  and  $F_{ij}$  in the Tsai-Wu failure criterion
    - $F_i$  and  $F_{ij}$  are derived directly from the material strength properties
    - $F_{12}$  can be adopted for the different types of materials used in the analyses
      - \*  $F_{12}(1)$  for material type number 1 (undamaged)
      - \*  $F_{12}(2)$  for material type number 2 (matrix failure)
4. Selective parameters:
  - parameter  $\beta$ , to decide which type of failure is assumed to occur
  - Output parameter  $\Delta ff$ , deciding whether ultimate failure has been reached

The material strength and stiffness properties are treated here as parameters, because certain adjustments with respect to the experimentally determined values are justified in view of the limited accuracy of the experimental data. Moreover, the experimental setting for the biaxial testing (force-controlled) differed from the procedure for obtaining the uniaxial strength data (displacement-controlled).

The computational results for the successive loading steps have been evaluated by counting the elements where matrix failure or fibre failure did occur. From these numbers, the development of damage can be resolved.

One of the major output parameters that we use, is the total number of layers in which fibre failure does occur. An extra-ordinary increase of the total number of layers with fibre failure will be

considered as ultimate laminate failure (ULF). Parameter  $\Delta ff$  is defined as the value taken for this extra-ordinary increase.

There is of course a direct relation between the area covered by elements where fibre failure will occur and the mesh refinement (defined by parameter  $mf$ ). With a higher mesh refinement, more elements will fail at the same time within a comparable area. This will effect both the number of elements where first-fibre failure did occur and the increase of the number of elements that failed through fibre failure.

We use the initial uniaxial strengths and the average stiffness to compute all types of biaxial testing with different values for the parameters  $mf$ ,  $\beta$ ,  $F_{12}(1)$  and  $F_{12}(2)$ .

As an example, the comparison between computational and experimental results for laminate type A are depicted in Figure 4.1 for a specific combination of parameters.

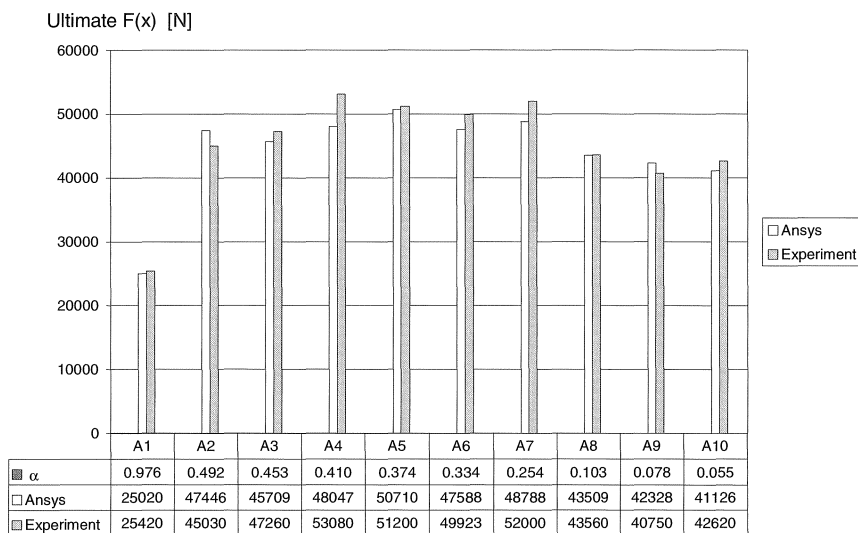


Fig. 4.1 Bar graph comparing computational and experimental results for parameter set:  $\beta = 20$ ,  $F_{12}(1) = 0$ ,  $F_{12}(2) = 0$ ,  $mf = 3$ ,  $\Delta ff = 3$ . ( $\alpha = F_y / F_x$ )

These results show that our computational tool is able to follow the deformation and progressive failure behaviour of composite laminates.

In order to illustrate the agreement between computational and experimental results, both results (taken from the biaxial experimental result of a particular test) are compared with respect to the evolution of the tensile force  $F_x$  as a function of the strain in the x-direction.

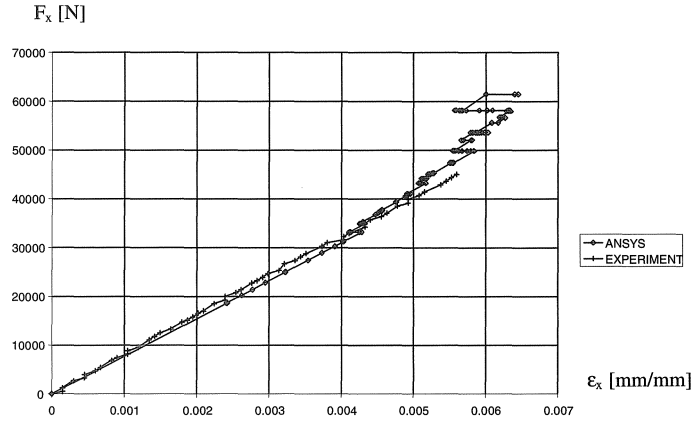


Fig. 4.2 Comparing Ansys computational and experimental results for a specific biaxial test ( $\alpha = 0.49$ ).

For this comparison, we adopt the average strain computed at the integration points coinciding with the area of the attached strain gauges as the computational strain.

The agreement between the experimental results and the corresponding computational analysis is remarkably good, as illustrated in Figure 4.2. The Ansys analysis was performed up to a level where the overall computational damage is very high. At this level, the material in the computational model is still capable to transfer loads carried by the remaining intact part of the structure. The real specimen, however, will fail immediately at this point, because of the limitations of force-control in the closed loop testing circuit.

## 5 Design of a vertical storage vessel

As an example of the importance of progressive failure analysis, we consider a cylindrical storage vessel in a GRP-laminate (thickness  $t$ ).

The cylindrical shell is clamped to a bottom plate.

All problems of symmetrical deformation of circular cylindrical shells can be reduced to the integration of Equation (5.1).

$$\frac{d^2}{dy^2} \left( K \frac{d^2 w}{dy^2} \right) + \frac{Et}{a^2} w = Z \quad (5.1)$$

where  $K = \frac{Et^3}{12(1-\nu^2)}$  is the flexural rigidity of the shell, and  $Z$  the pressure normal to the surface of the cylinder.

For a shell with constant thickness and using the notation

$$\lambda^4 = \frac{Et}{4a^2 K} = \frac{3(1-\nu^2)}{a^2 t^2} \quad (5.2)$$

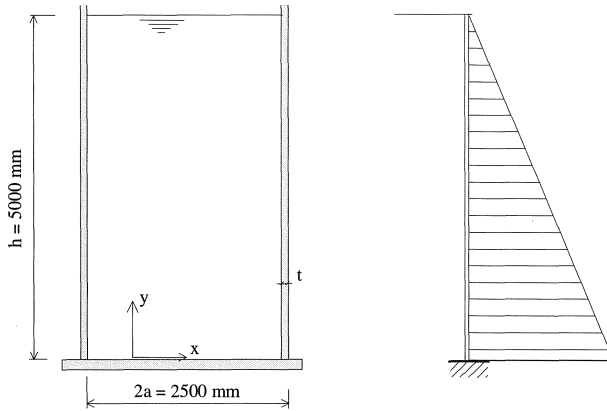


Fig. 5.1 Vertical storage vessel loaded with internal hydrostatic pressure.

Equation (5.1) can be presented in the simplified form:

$$\frac{d^4 w}{dy^4} + 4\lambda^4 w = \frac{Z}{K} \quad (5.3)$$

This is the same equation as obtained for a prismatic bar with a flexural rigidity  $K$ , supported by a continuous elastic foundation and submitted to the action of a load of intensity  $Z$ . The spring constant of the elastic foundation is

$$k = \frac{Et}{a^2}.$$

An approximation of the elastic solution can be found assuming a constant pressure equal to the pressure at bottom level ( $p_0 = \rho gh$ ) and so neglecting the height dependency of the hydrostatic pressure.

The general solution of Equation (5.3) can be written as:

$$w = A e^{-\lambda y} \sin(\lambda y + \omega) + \frac{p_0}{k} \quad (5.4)$$

With edge conditions: ( $y = 0; w = 0$ ) and ( $y = 0; \frac{dw}{dy} = 0$ ) it follows:

$$A = -\frac{p_0 \sqrt{2}}{k}; \quad \omega = \frac{\pi}{4}$$

so the general solution is:

$$w = -\frac{p_0 \sqrt{2}}{k} e^{-\lambda y} \sin\left(\lambda y + \frac{\pi}{4}\right) + \frac{p_0}{k} \quad (5.5)$$

Substituting this solution for  $w$  in the expression for the bending moment:

$$M_y = -K \frac{d^2 w}{dy^2} \quad (5.6)$$

it follows that:

$$M_y = \frac{p_0 \sqrt{2}}{2\lambda^2} e^{-\lambda y} \sin\left(\lambda y - \frac{\pi}{4}\right) \quad (5.7)$$

The solutions in Equation (5.5) and Equation (5.7) are valid for isotropic materials.

In order to determine the general solution for an anisotropic material, the coefficients in the differential equation have to be adapted.

The expressions for  $K_y$  and  $k$  can be rewritten as:

$$K_y = \frac{1}{12} \frac{E_y t^3}{(1 - \nu_{yx}^2)} \quad \text{and} \quad k = \frac{E_x t}{a^2}$$

So:

$$\lambda^4 = \frac{k}{4K} = \frac{E_x t}{\frac{1}{3} \frac{E_y t^3 a^2}{(1 - \nu_{yx}^2)}}$$

and

$$\lambda = \frac{\sqrt[4]{3E_x(1 - \nu_{yx}^2)}}{\sqrt{at}} \frac{E_y}{E_y} \quad (5.8)$$

The height of the bottom area where the bending stresses are not negligible, depends on the thickness and the composition of the laminate used.

In order to show the effects of the choice of a laminate, we will apply a laminate similar to type A in the x-direction (*design I*) and in the y-direction (*design II*), respectively.

For the initial design, eight layers of 0.5 mm thickness are applied with laminate lay-up  $(0^\circ, +45^\circ, -45^\circ, 0^\circ)_s$ .

The elastic constants for laminate *design I* and *design II* are, respectively:

*design I*:  $E_x = 17216$  MPa,  $E_y = 7860$  MPa and  $\nu_{yx} = 0.236$ .

*design II*:  $E_x = 7860$  MPa,  $E_y = 17216$  MPa and  $\nu_{yx} = 0.517$ .

The results of  $m_y$  (bending moment per unit of width) for both laminate types have been depicted in Figure 5.2.

In Figure 5.3, the radial displacement is depicted for  $p_0 = 0.05$  MPa.

From the distribution of  $m_y$  and  $u_r$  it may be concluded that for heights beyond 500 mm the influence of the edge has disappeared.

We will confine the progressive failure analysis to the bottom area of the vessel where the edge disturbances are clearly not negligible.

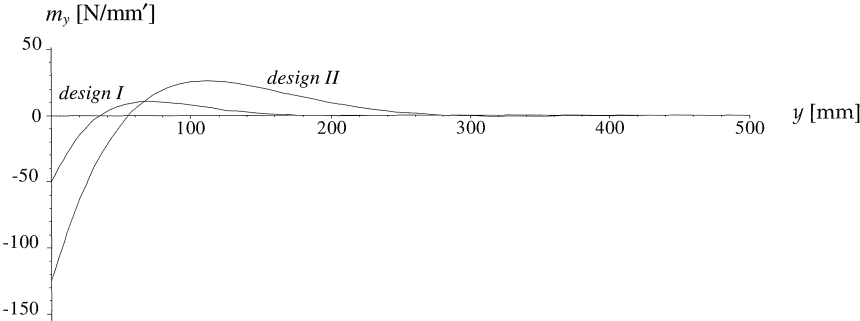


Fig. 5.2 Bending moment distribution in bottom area for a type A laminate applied in the x-direction (design I), and in the y-direction (design II).

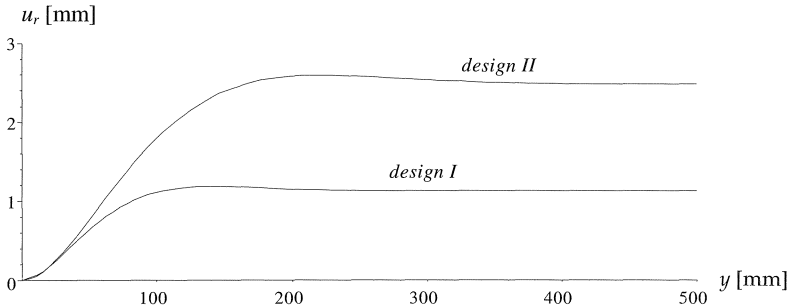


Fig. 5.3 Radial displacement in bottom area for a type A laminate applied in the x-direction (design I), and in the y-direction (design II).

A progressive failure analysis has been performed on the finite element model of a small vertical cut-out of the cylindrical vessel. The lowest area ( $h'$  up to 500 mm) is provided with elements suited to progressive failure analysis. The elements in higher regions will not be allowed to degrade during the analysis. The results of two analyses (design I and design II, respectively), expressed in the minimum and maximum moments, are depicted in Figure 5.4 for increasing hydrostatic pressure:

$$n_p = \frac{p_{\text{progressive}}}{p_0} \tag{5.9}$$

The increase of the moment during the progressive failure development is quite different for both laminate types.

For *design II* we see a considerable increase of  $m_y$  (max) and  $m_y$  (min) when first-ply failure occur; this increase is not present in the analysis at the first-ply failure level for *design I*.

Defining FPF as the value where first-ply failure occurs and FFF as first-fibre failure, the FFF/FPF quotient can be used as a measure for the failure capacity above the level of first-ply failure.

The FFF/FPF quotient is dramatically low for *design II* ( $4.88/3.43 = 1.4$ ) compared with *design I* ( $9.69/2.92 = 3.3$ ).

These results will clearly lead to a drastic difference with respect to the required vessel thickness for both designs (in favour of *design I*).

Investigation of other than the used stacking sequences in a type A laminate and other laminate compositions, of course, could lead to an even more favourable result.

More generally, the example shows that the use of the progressive failure analysis has the potential of resulting in an optimal laminate design.

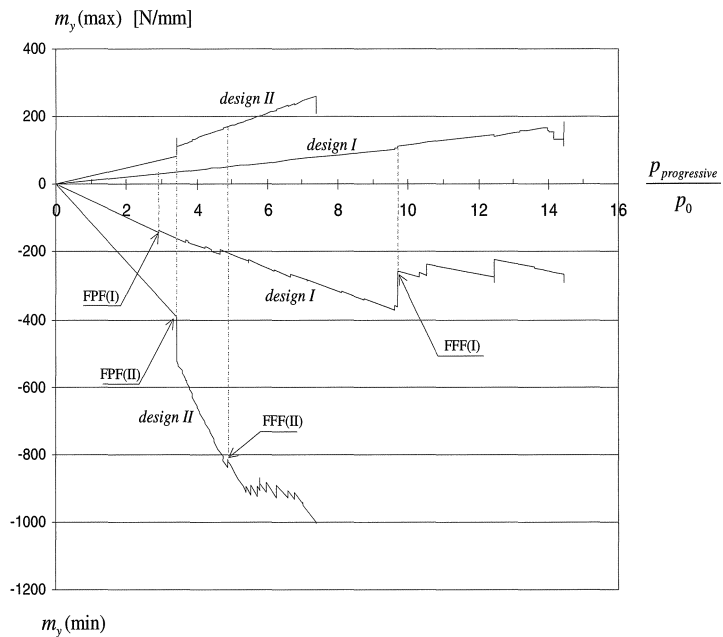


Fig. 5.4 Progressive failure analysis of design I ( $90^\circ, +45^\circ, -45^\circ, 90^\circ$ )<sub>s</sub> and design II ( $0^\circ, +45^\circ, -45^\circ, 0^\circ$ )<sub>s</sub>.

## 6 Conclusions

We have developed a finite element computational tool for simulating progressive failure and ultimate performance of laminates, based on the deformation and failure mechanisms per unidirectional layer.

The reliability of this computational tool is verified by biaxial experiments on glass-fibre polyester laminates. Despite the use of a rather simple procedure to select the type of failure that will occur at any stage of loading, the computational procedure proved capable of reasonably predicting ultimate failure.

Referring specifically to the results of a biaxial test session where strain gauges were used (Figure 4.2), the agreement between the experiment and the computational analysis was remarkably good for a final set of parameters.

Successive failure stages were computed for various laminate types and loading ratios using several parameter combinations.

The best agreement between the computational and the experimental results for different loading ratios is achieved for a specific laminate with three fibre directions (type A) and with the following set of parameters:  $mf = 3$ ,  $\beta = 20$ ,  $F_{12}(1) = 0$  and  $F_{12}(2) = 0$ .

The computational agreement for laminates with less than three fibre directions is not perfect.

The computational results over-estimate the experimental results. A major reason for this is quite likely the harmful effect of transverse inter-laminar stresses near the edge of the centre hole, where failure is initiated. These stresses have to be quantified yet in order to proof the statement above.

It may be stated, however, that laminates with more than two fibre directions will be applied quite generally in structural applications that are subjected to a biaxial state of stress. Thus, the deviation for two-directional laminates is not too relevant.

The chosen mesh refinement will certainly affect the overall result of a progressive failure analysis. There will be an optimal mesh refinement for any structure, correlated with the available computation time and the aimed exactness of the solution.

Our aim has been to show that our finite element computational tool, using the Tsai-Wu failure criterion for the unidirectional layer, is able to follow the deformation and progressive failure behaviour of composites. The comparison between experimental and computational results shows that we have been successful in that respect.

## List of Symbols

$a$	Cylinder radius
$a_{im}$ etc.	Cosine
$c_{ijkl}$	Stiffness tensor elements
$\tilde{c}_{ijkl}$	Transformed stiffness tensor elements
$c_{ij}, \bar{c}_{ij}$	Stiffness tensor elements, contracted notation
$C_{ijkl}$	Stiffness tensor
$\tilde{C}_{ijkl}$	Transformed stiffness tensor
$C_{ij}, \bar{C}_{ij}$	Stiffness tensor, contracted notation
$E_x, E_y$	Moduli of elasticity (multidirectional laminate)
$E_1, E_L$	Modulus of elasticity in the fibre direction (unidirectional layer)
$E_2, E_T$	Modulus of elasticity perpendicular to the fibre direction (unidirectional layer)
$E_f$	Modulus of elasticity of fibre material
$E_m$	Modulus of elasticity of matrix material
$F_x, F_y$	Forces in the x- and y-direction
$F_{ij}, F_i$	4th and 2nd-order strength tensor (contracted notation)
$G_{12}, G_{LT}$	Shear modulus of unidirectional layer in the symmetry direction
$k$	Elastic spring constant
$K$	Flexural rigidity (isotropic)
$K_x, K_y$	Flexural rigidity (anisotropic)
$mf$	Mesh frequency
$m_y$	Bending moment per unit of width
$M_x, M_y$	Bending moments
$s_{ijkl}$	Flexibility tensor elements
$\tilde{s}_{ijkl}$	Transformed flexibility tensor elements
$s_{ij}, \tilde{s}_{ij}$	Flexibility tensor elements, contracted notation
$S$	Shear strength of unidirectional layer
$Sf$	Safety factor
$S_{ijkl}$	Flexibility tensor, compliance tensor
$\tilde{S}_{ijkl}$	Transformed flexibility tensor
$S_{ij}, \tilde{S}_{ij}$	Flexibility tensor, contracted notation
$t$	Laminate thickness
$t_k$	Thickness of layer $k$
$u$	Subscript (ultimate)
$u_x, u_y$	Displacement in the x-direction, etc.
$v_f$	Volume fraction of fibres
$v_m$	Volume fraction of matrix
$X_t$	Tensile strength of unidirectional layer in the fibre direction
$X_c$	Compressive strength of unidirectional layer in the fibre direction
$Y_t$	Tensile strength perpendicular to the fibre direction (unidirectional layer)
$Y_c$	Compressive strength perpendicular to the fibre direction (unidirectional layer)
$\alpha$	Loading ratio in biaxial testing
$\beta$	Selective parameter
$\Delta ff$	Computational parameter
$\epsilon_{ij}$	Strain tensor
$\epsilon_i$	Strain tensor (contracted notation)
$\theta$	Rotation angle
$\Pi_1, \Pi_2$	Level of stresses in stress criterion

$\kappa$	Curvature
$\sigma_{ij}$	Stress tensor
$\sigma_i$	Stress tensor (contracted notation)
$\sigma_{xu}, \sigma_{yu}$	Ultimate (yield) stress in the x-direction (anisotropic), etc.
$\tau_{xyu}$	Ultimate (yield) shear stress
$\nu_{ij}$	Poisson's ratio
$\xi_s$	Inverse strength ratio

## References

1. AGARWAL, B. D. and L. J. BROUTMAN  
Analysis and Performance of Fiber Composites  
*John Wiley & Sons, Inc, 1990*
2. BULL, J.W. (editor)  
Numerical Modelling of Composite Materials  
*Chapman & Hall, London, 1996*
3. CHANG F. K. and K.Y. CHANG  
A Progressive Damage Model for Laminated Composites containing Stress Concentrations.  
*Journal of Composites Materials, vol.21, p834-855, 1987*
4. COATS, T. W. and C. E. HARRIS  
Experimental Verification of a Progressive Damage Model for IM7/5260 Laminates Subjected to Tension-Tension Fatigue  
*Journal of Composite Materials, vol.29, no.3, 1995*
5. DANIEL, I. M. and C. L. TSAI  
Analytical/Experimental Study of Cracking in Composite Laminates under Biaxial Loading  
*ICCM/8 Hawaii, 37-C.1-37-C.10, 1991*
6. JEN, K.C. and K. MAO  
Modelling Progressive Failure in Laminated Composites  
*Proceedings of ABAQUS users conference, Newport. Hibbit, Karlsson and Sorensen Inc., Pawtucket, RI, 1992*
7. KIM, J. K. and D. S. KIM  
Notched Strength and Fracture Criterion in Fabric Composite Plates Containing a Circular Hole  
*Journal of Composite Materials, vol.29, no.7, 1995*
8. KUO-SHIH LIU and S.W. TSAI  
A Progressive Quadratic Failure Criterion for a Laminate  
*Composites Science and Technology, vol.58, pp.1023-1032, 1998*
9. LEE J. W. and I. M. DANIEL  
Progressive Transverse Cracking of Crossply Composite Laminates  
*Journal of Composite Materials, vol.24, pp.1225-1243, 1990*

10. PUCK, A.  
Zum Deformationsverhalten und Bruchmechanismus von Glasfaser/Kunststoff  
*Kunststoffe Bd 55, 913, 1965*
11. SENDECKYJ, G. P.  
A Brief Survey of Empirical Multiaxial Strength Criteria for Composites  
*Composite Materials: Testing and Design (Second Conf.), ASTM STP 497, 1971*
12. SENDECKYJ, G. P. (editor)  
Composite Materials, Vol.2: Mechanics of Composite Materials  
*Academic Press, New York and London, 1974*
13. SHAHID, I. and F. K. CHANG  
An Accumulative Damage Model for Tensile and Shear Failures of Laminated Composite Plates  
*Journal of Composite Materials, vol.29, no.7, 1995*
14. SHIH, G. C. and A. M. SKUDRA (editors)  
Failure mechanics of composites  
Handbook of Composites, Vol. 3  
*Elsevier Science Publishers bv., Amsterdam, 1985*
15. SLUIMER, G. M.  
Experimental Evaluation of Failure Criteria applied to Multi-directional Laminates of Glass-fibre Reinforced Polyester  
*ICCM-9 Proceedings, Volume VI, pp. 907-912, 1993*
16. SLUIMER, G. M.  
Evaluation of strength of laminates in a biaxial state of stress, by means of a selective progressive failure criterion  
*ICCM-10 Proceedings, Volume V, pp. 187-193, 1995*
17. SLUIMER, G. M.  
Ultimate Performance of GRP-Laminates under in-plane Biaxial Loading  
Dissertation Delft University of Technology, Delft, The Netherlands, 1998  
*ISBN 90-407-1802-4 / CIP*
18. TAN, S.C.  
A progressive failure model for composites plates containing openings  
*Journal of Composite Materials 25, 556-577, 1991*
19. THOM, H.  
A Review of the Biaxial Strength of Fibre-reinforced Plastics  
*Composites part A, vol.29, no.8, 1998*
20. TSAI, S. W.  
A Survey of Macroscopic Failure Criteria for Composite Materials.  
*Journal of Reinforced Plastics and Composites, vol 3, pp.40-62, 1984*
21. TSAI, S. W. and E. WU  
A General Theory of Strength for Anisotropic Materials  
*Journal of Composite Materials, Vol.5, p.58, January 1971*

22. TSAI, STEPHEN W. and H. THOMAS HAHN  
Introduction to Composite Materials  
*Technomic, 1980*
23. WHITNEY, J. M. and R. J. NUISMER  
Stress Fracture Criteria for Laminated Composites Containing Stress Concentrations  
*Journal of Composite Materials, Vol.8, July 1974*
24. WU, E.M.  
Phenomenological Anisotropic Failure Criteria of Composite Materials  
In: Vol.2: Mechanics of Composite Materials, (Ed. Sendekyj, G.P.), pp. 353-431.  
*Academic Press, New York and London, 1974*